In-depth Observations on the Formation and Disintegration of a Cluster Microform

K.G. Heays[1], H. Friedrich[1] and B.W. Melville[1]
[1]Department of Civil and Environmental Engineering,
The University of Auckland
Auckland 1021
NEW ZEALAND
E-mail: khea021@aucklanduni.ac.nz

Abstract: *A laboratory study was conducted to observe the particle movements that create a cluster microform, measure the dimensions of the cluster then detect the influence the cluster has on the sediment in the remainder of the bed. Experiments were undertaken in a laboratory flume using well graded rounded river gravels ranging in diameter from 1 - 30 mm. A well defined, stable cluster was created in the test environment. Continuous image recording for the duration of the experiment allowed monitoring of the cluster formation and disintegration. Particle tracking was utilised to give the particle movement within and around the cluster and image analysis was used to record cluster dimensions. These tools showed that the stoss size was similar to the anchor stone size for most of the period where the cluster was formed. The size of the wake fluctuated significantly and the cluster orientation was observed to remain within 6^o of the streamwise direction while the cluster was fully formed. The particle mechanics leading to the formation and disintegration are highlighted, providing insight into the dependence of the cluster stability on the surrounding bed. Measurements of the sediment transport rates showed a reduction in the localised peak rates while the cluster was formed, and increased again after the cluster disintegrated.*

Keywords: *Cluster formation, Armouring, Sediment transport, Photogrammetry, Image processing*

1. INTRODUCTION

Cluster microforms have been shown to play an important role in the stabilisation of river beds (Church et al. 1998; Oldmeadow and Church 2006). Their formation provides added resilience to a river bed, and they have been shown to withstand flows of up to twice the critical condition (T_{cr}*) (Church et al. 1998). The formation of clusters is the result of complex interactions between the flow field and the river bed and has been attributed to the selective transport of grains either through turbulent fluctuations or varied grainsize (Strom 2006). Clusters play an integral role in riverbed dynamics; their relative stability enables them to provide shelter for local periphyton, invertibrates and fish (Biggs et al. 1997) and their effect on sediment transport rates makes them an important factor in sediment load prediction. A complete understanding of the cluster life cycle is therefore important in improving river engineering practices, in-stream habitat protection and sediment transport prediction.

Typically a cluster consists of an unusually large anchor stone, an upstream deposition of medium sized particles termed the ‘stoss’, and a deposition of finer particles behind the anchor stone, termed the ‘wake’ (Brayshaw 1984). Additional to this typical cluster structure, other cluster arrangements have been identified, which consist of particles grouping together in stable arrangements, such as a ‘line’, ‘heap’, ‘comet’, and ‘ring’ (Strom and Papanicolaou 2008). Cluster occurrence was originally attributed to sediment grading and particle shape, where non-uniform sediment is more likely to form clusters (Reid et al. 1992). While this is an important factor, it has been proven that uniformly sized and shaped sediments are also able to form clusters (Papanicolaou and Schuyler 2003). Other factors influencing cluster formation are sediment availability, specific gravity, and flow intensity (Papanicolaou and Schuyler 2003).

Strom and Papanicolaou et al. (2004) classified cluster evolution under increasing flow as occurring in three phases with respect to the flow sediment interaction. In Phase I, the clusters act as sediment sinks, with passing suspended sediment being trapped in the cluster formation. Phase II is an intermediate stage, where clusters have reached their maximum size, but have not started to disintegrate. This stage has no effect on the bedload rate of the river. Phase III is the stage where clusters start to disintegrate. At this stage they become a source of sediment, increasing the mean bedload rate as sediment from the less stable areas of the cluster, such as the wake, is released until the entire cluster has disintegrated. Brayshaw (1984) postulated that cluster break up was dependent on the calibre of the anchor stone, whereas De Jong (1991) found that cluster breakup was dependent on the overall cluster morphology. A recent study has observed both methods of disintegration, with sediment distribution playing a significant role in the cluster behaviour (Hendrick et al. 2010). Bimodal sediment was found to be more stable and subject to disintegration only once the anchor was dislodged, and uniform sediment was found to disintegrate at lower stresses while leaving the anchor stone in place (Hendrick et al. 2010) to become the foundation for a new cluster.

Investigation into the formation of clusters has been steady over the last few decades, with a number of both river and laboratory studies having been conducted. In laboratory experiments, the emergence of photogrammetry has provided researchers with a versatile new tool for examining sediment behaviour during high flows (Heays et al. 2010a; Heays et al. 2010b; Kramer and Papanicolaou 2005; Papanicolaou et al. 2003). Because of the complex nature of cluster formation, the insights that can be made through photogrammetry are valuable in determining the mechanics behind their formation and disintegration.

This paper presents the findings from continuous photographic observation of a well graded, static, gravel bed, at a constant flow rate. This provides insight into cluster formation in a more realistic environment than that of idealized spherical beads. In this experiment, a stable cluster was observed to form, the physical boundaries of which have been recorded as the cluster formed and eventually disintegrated. The individual movements of particles involved in the formation of the cluster are also presented, as are the sediment transport rates of the bed surrounding the cluster.

2. METHOD

Experiments were conducted in the Hydraulics Laboratory at The University of Auckland. The flume used is 0.45 m wide, 0.45 m deep and 19 m long. The test section comprised of a fixed bed with a vertically adjustable recess filled with rounded river gravels. The sediment recess was 0.95 m long, 0.45 m wide and 0.1 m deep. The bed was water worked for 271 min at a constant flow rate. A velocity profile was taken upstream of the test section; the average velocity was u_{av} = 0.993 m/s and bed shear velocity u^* = 0.084 m/s. The shear velocity was approximately equal to the critical shear velocity of the D_{50} (grainsize at which 50% of the bed is finer), using $\theta_c = 0.0834(d_i/d_{50})^{-0.872}$ (Andrews 1983).

The sediment was well graded, with D_{98} = 25 mm, D_{50} = 4.5 mm, and D_{16} = 1.5 mm. The gravel was initially manually mixed and placed into the sediment recess of the flume, so that it lay flush with the false floor. There was no sediment supply, but the floor of the recess was raised slowly to ensure the upstream end of the test section was flush with the upstream false floor at all times. The gravel in the test section was separated into five size groups, with each group painted a different colour to enable identification of different sized particles. Thresholds for size groups were chosen to be D_{38}, D_{55}, D_{80} and D_{98}, of the subsurface grading curve. These values roughly correspond to the sizes of particles in the stoss and wake of a cluster. Before the experiment commenced, a larger particle was placed on the surface of the test section. This particle was intended to act as an anchor stone and initiate a cluster formation. The anchor stone had mutually perpendicular dimensions, L = 64 mm, I = 42 mm and S = 18 mm, and lay with the L dimension transverse to the flow and S dimension vertical. The stone can be described as slightly elongate and moderately flat (Blott and Pye 2008).

Plan view images of the bed surface were continuously taken at approximately 1 frame per second, using a Nikon D90 camera. To enable capture of a clear image of the surface sediment, a Perspex skimmer was fabricated to eliminate surface waves and ripples. The skimmer was vertically adjustable to enable it to sit lightly on the water surface. Matlab was used for all of the image processing and analysis of the photographs. Images were loaded into Matlab and calibrated for processing. The different colours were isolated enabling work with individual size fractions. A particle tracking algorithm was developed based on image subtraction between subsequent frames, allowing identification of any particles which moved between frames. Particles were matched according to their proximity, similarity of size, aspect ratio, and conformation with a number of size and distance related limits (Heays et al. 2010b). The larger two size fractions were successfully tracked. In a 100 frame accuracy test, 100% accuracy was achieved for the largest fraction, and 88% positive detection and 1.5% false detection were achieved for the second largest fraction. Tracking accuracy was much diminished for smaller sizes due to their more dispersed nature and the frame rate which was not fast enough to capture a manageable amount of particles to track.

Identification of the stoss and wake portions of the cluster was achieved through the assumption that any large particles directly upstream of the anchor stone were a part of the stoss, and any small particles directly downstream of the anchor stone were a part of the wake. The movements of any larger sized particles entering, leaving or influencing the cluster region were also recorded.

3. RESULTS

3.1. Cluster formation and disintegration

As a result of the protrusion of the anchor stone at the start of the experiment, the stone was entrained a small distance, and repositioned at an angle to the horizontal (Figure 1a, Figure 1b). The angle of the anchor stone in its new position provided a sheltered area behind the anchor stone where smaller particles deposited, forming the wake.

Subsequent to the initial movement of the anchor stone, the spatial boundaries of the cluster were chartered. The stoss and wake regions have been outlined and superimposed over the corresponding image of the bed. Immediately after the anchor stone deposited, a large wake region formed (Figure 2a). It then quickly diminished (Figure 2b) and fluctuated around this size for the remainder of the experiment. The size of the wake is much less dependent on the surrounding bed than the stoss; it is more likely to form as a direct response to the low pressure zone created behind the anchor stone. It is large at the beginning of the experiment, but as time passes, fluctuations in the flow entrain particles at rest which are less readily replaced. Figure 2b shows the first particles joining the anchor stone to create the cluster, Figure 2c shows the cluster with the stoss fully formed, and Figure 2d shows the cluster immediately after the stoss disintegrates. This information was gathered for each frame for the duration of the experiment, allowing quantification of the cluster size over time.

Figure 3 shows the size of the stoss (Figure 3a) and wake (Figure 3b) relative to the size of the anchor stone (which stays constant). Figure 3a shows a very clear period where the stoss is well formed between minutes 113 and 240. Overall, the size of the stoss is similar to the size of the anchor stone, with a sharp peak at the initiation of the cluster and a gradual decrease in size. Prior to the complete stoss formation there is a gradual increase in stoss size, and subsequent to cluster disintegration the stoss area drops to zero but begins to increase again, possibly forming the beginning of a new cluster. The formation of the wake is less well defined, showing significant fluctuation throughout the experiment. Corresponding with the time at which the anchor stone is deposited to its new position, the initial size of the wake quickly grows to twice the size of the anchor stone. The wake then reduces and fluctuates significantly. During the period where the stoss is formed, the wake shows an increase in size. This occurs between minute 124 and 170. The size of the wake rises from around 0.25 of the anchor stone size to closer to 0.75, with peaks reaching 1.5 and 2, times the anchor stone size. At its maximum, the overall size of the cluster is 4.5 times the anchor size, which equates to approximately 2% of the total test section area.

The orientation of the cluster (Figure 4) was determined as the angle between the streamwise axis and the long axis of the ellipse that encloses the cluster. As can be seen in Figure 4a, the angle of orientation of the cluster is meaningless before the cluster is formed. Once formed, it can be seen that from minute 125, the orientation becomes more constant. While still fluctuating, the orientation is generally close to 0^o. The angle of orientation during the period when the cluster is well formed is shown in Figure 4b. This shows that while the cluster is fully formed, the majority of the time the orientation is within 6^o of the streamwise direction.

The formation and disintegration of the cluster occurred despite the flow rate of the experiment remaining the same for the duration of the experiment. A number of studies have predicted cluster formation cycles to follow the form of the cluster growing with increasing shear stresses, and disintegrating once the shear stress becomes too great (Papanicolaou and Schuyler 2003; Papanicolaou et al. 2003; Strom et al. 2004). Other studies have reported that clusters form on the waning arm of a flood (Brayshaw 1984; De Jong 1991; Hassan and Reid 1990). This study shows that a cluster microform can form, remain stable and then disintegrate at the same average flow.

The general formation process of the cluster followed a similar regime as observations made by Brayshaw (1984); the wake was the first part of the cluster to form, and stoss deposition only occurred after a fairly long period of time had passed. The deposition of one or two stoss particles appeared to assist the deposition of more particles. A large wake was observed to form immediately after anchor stone deposition, then diminish, and become larger only once the stoss formed. This has not been reported in other cluster observations, but can be explained. Wake particles have been found to have a higher transport rate than stoss particles which has been attributed to bursts in the vortex behind the anchor stone (Billi 1988; Wittenberg and Newson 2005). This may entrain the particles which settled quickly in the wake, diminishing them over time. The addition of stoss stones to the anchor would increase the size of the obstacle, in turn increasing the size of the low pressure zone which allows wake particles to settle, and growing the size of the wake while the cluster is fully formed.

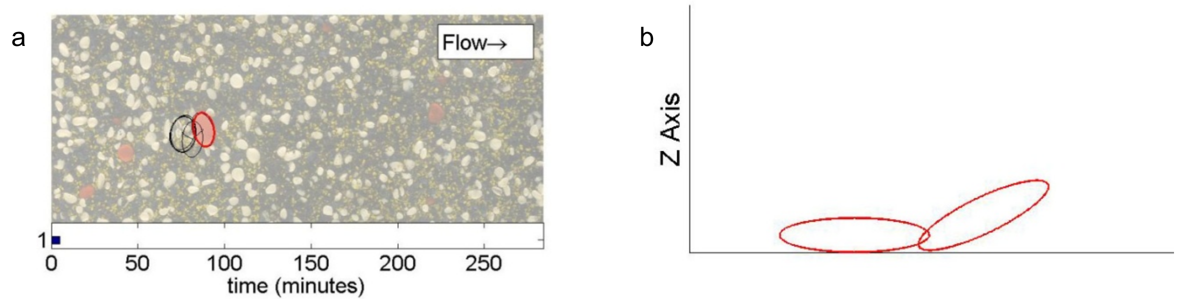

Figure 1 Anchor stone positioning over the first 5 minutes a) Plan view on test bed b) Side view

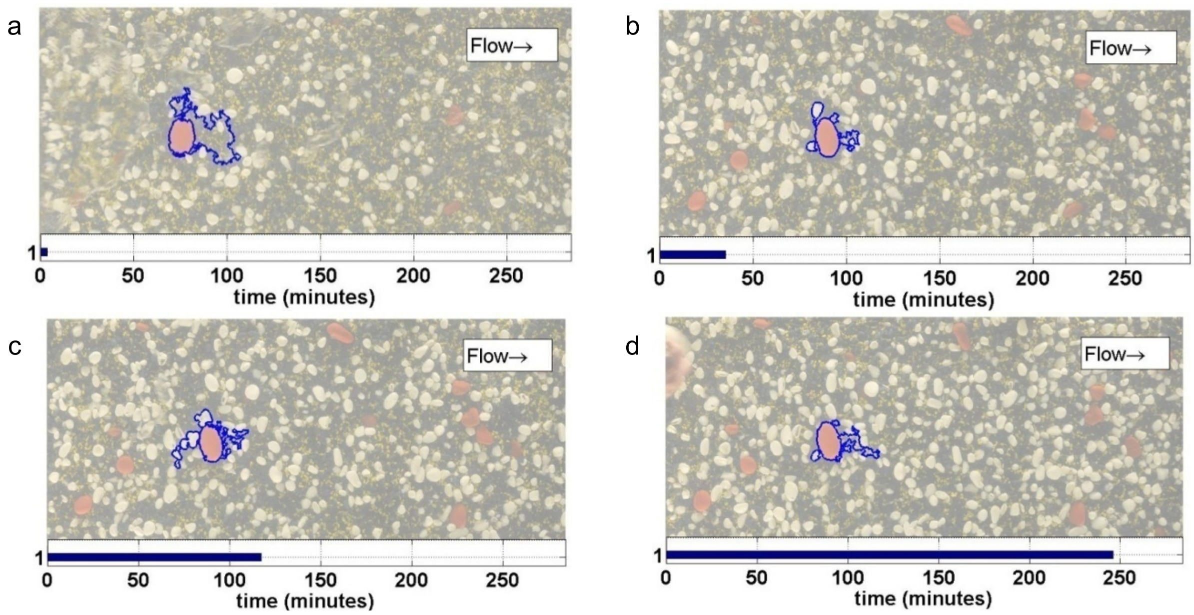

Figure 2. Life cycle of the cluster

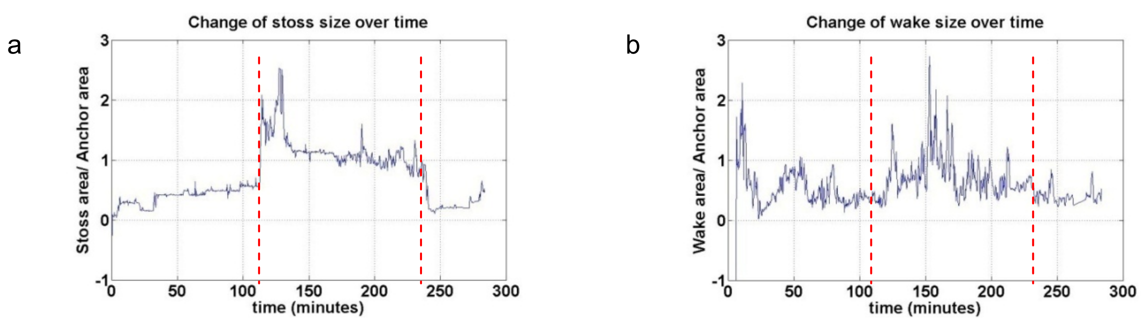

Figure 3. Size of stoss (a) and wake (b) over the duration of the experiment (dashed lines showing time when cluster is fully formed)

a

b

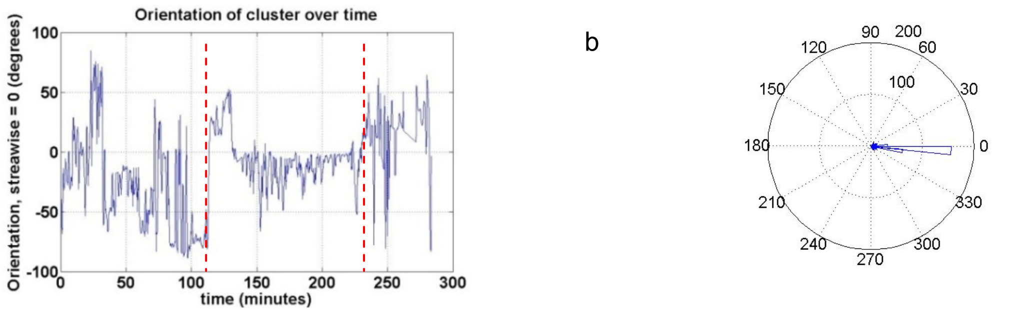

Figure 4. Orientation of cluster (a) over the duration of the whole experiment (dashed lines highlighting the time when the cluster is fully formed) (b) when fully formed

Particles with a significant involvement in the cluster forming process were identified through observation. Each particle was then tracked to determine its position and orientation throughout the experiment. Using Figure 3a, the cluster process has been divided into three sections; formation, duration and disintegration. The particle movements during these three phases have been presented in Figure 5a, Figure 6a and Figure 6b. Figure 5a shows the migration of all particles which moved into the stoss region, while Figure 5b shows the movements of the stones which played a crucial role in the creation of the stoss. The process of formation was relatively long and was influenced by two significant events. The first event was the addition of a particle to the side of the anchor stone (Figure 5b black ellipse). The particle gradually moved toward the anchor stone in a sliding motion, this occurring over a period of around an hour and being shown on the timeline as the first segment of time. Once this first particle came to rest, the cluster became a barrier for entrained particles, increasing the likelihood of deposition into the stoss region. The second important event was the disintegration of another cluster directly upstream of the subject cluster. This released a number of particles, three of which settled in the heart of the stoss zone (Figure 5b white ellipses), also acting as a link to other particles slightly removed from the anchor stone. This occurred suddenly at minute 113. The particle movements relevant to the cluster subsequent to the stoss formation and prior to break up are plotted in Figure 6a. This 'duration phase' of the cluster shows that movement in the stoss region is relatively frequent. The cluster is stable, however particles move both into and out of the cluster during this period. After around 90 minutes, particles begin to move away, as shown in Figure 6b.

The initiation of the cluster disintegration is displayed in Figure 7, where all of the particles near the anchor stone were tracked over 2 minutes either side of the time of disintegration. The entrainment of a smaller particle to the side of the stoss (Figure 7b) is a precursor to the complete break up of the stoss, which happens less than thirty seconds later, and includes the entrainment of a nearby heap cluster to the side of the stoss (Figure 7c, Figure 7d). The small particle is entrained suddenly and with little disturbance to surrounding particles after remaining stationary for 15 minutes. Shortly after the entrainment of the first particle, the large stone directly upstream of the anchor, playing the role as the primary part of the stoss, moves slightly and is then entrained 1 second later with four other particles to the side of the cluster (Figure 7c). In the following few minutes, other particles in the cluster shift away from their resident positions, leading to disintegration of the cluster (Figure 7d). This observation of the cluster has shown that its formation and stability is dependent on other nearby clusters. The cluster is not necessarily a discrete formation, and may have similarities to the cell structures identified by Church (1998).

a

b

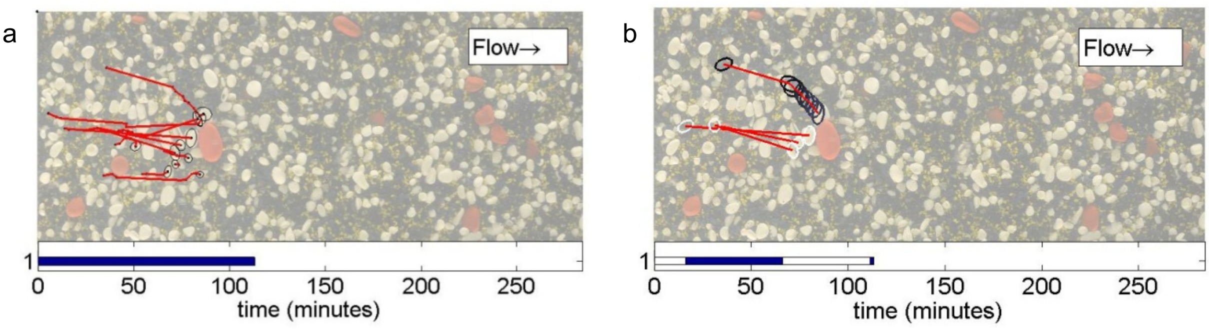

Figure 5 Formation of cluster: a) All particle movements involved in the formation of the stoss b) Two types of motion forming the stoss; sliding (black ellipse) and jump (white ellipses)

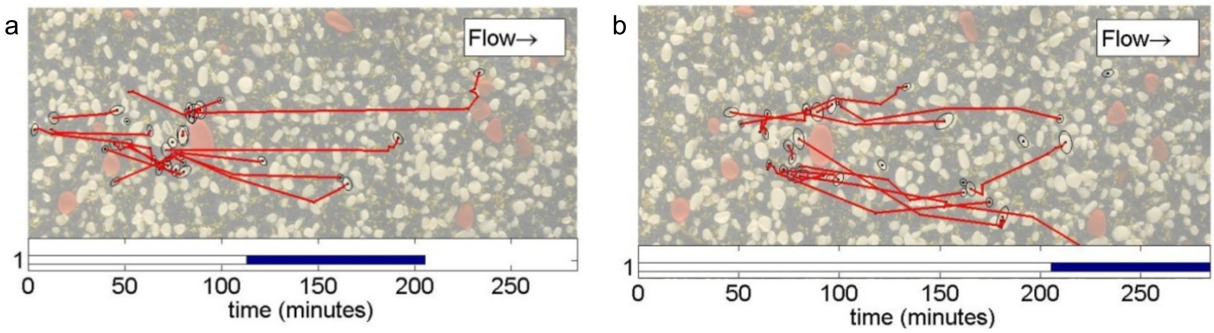

Figure 6. Duration and disintegration of cluster a) Particle movements during period when cluster was fully formed d) Cluster disintegration

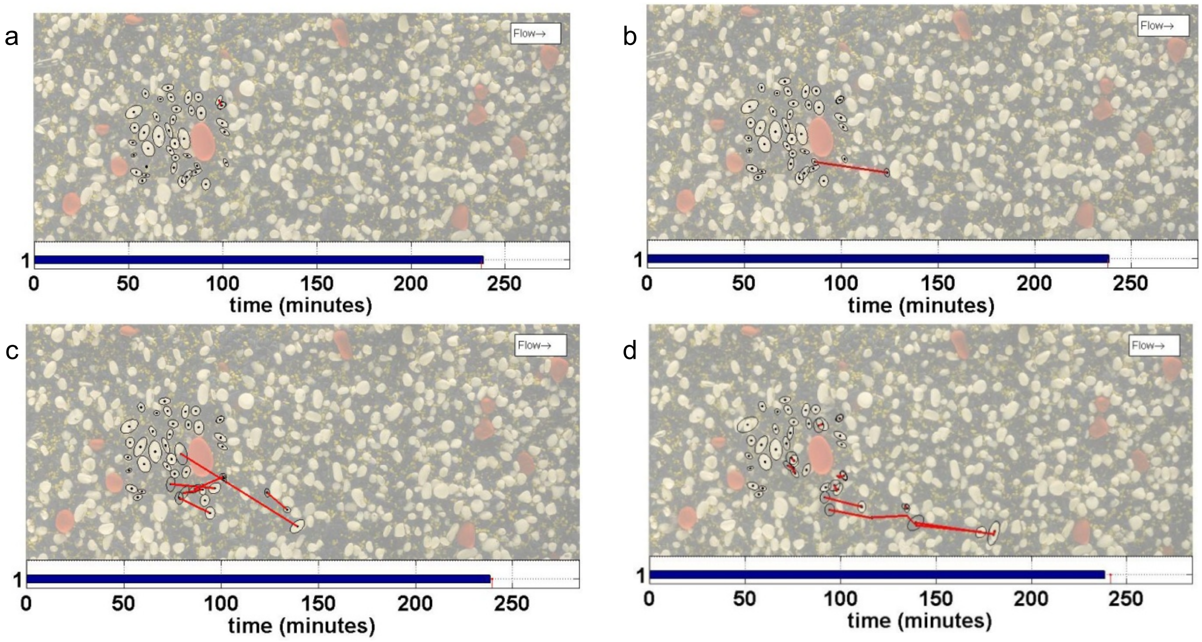

Figure 7. Cluster disintegration: a) Before break-up (t=237min) b) Entrainment of stone (t=237.5min) c) Disintegration of whole cluster (t=238 min) d) After disintegration (t =242 min)

3.2. Sediment transport

The sediment transport of larger size fractions of the surrounding bed was monitored over the duration of the experiment. This was then separated into the three primary stages in the cluster process. Also, the first 35 minutes of the experiment was separated in order to isolate the effects of armouring. Figure 8 shows the transport rate across the bed for the four stages; a) armouring (1-35 minutes) b) prior to cluster formation (35 – 110 minutes) c) cluster duration (110 -250 minutes) and d) subsequent to cluster breakup. The sediment transport rate was calculated by summing the volume of large (>9.5 mm) particles entrained from the bed. The total sediment transport rate for the bed in stage a) was 1.21 m^3/h, stage b) was 0.495 m^3/h, stage c) was 0.535 m^3/h and stage d) was 0.508 m^3/h. The spatial distribution of this sediment transport is depicted in Figure 8.

The armouring phase shows a distinct area of no sediment movement directly behind the stoss. This corresponds to the wake, which is formed in this area, resulting in only finer particles moving in this zone. Transport rates quickly diminish after the first 35 minutes, and Figure 8b shows only two regions of transport, one directly upstream of the cluster, and the other downstream of the cluster. Figure 8c implies that during the period where the cluster is fully formed, peak transport rates are lower than when the cluster is non-existent. There is a particularly noticeable reduction in transport rates downstream of the cluster, with peak localised transport rates dropping to less than 0.01 m^3/hr. After cluster disintegration, peak localised transport rates increase again to up to 0.02 m^3/hr in localised areas and the zone of high transport downstream of the cluster increases in activity once again.

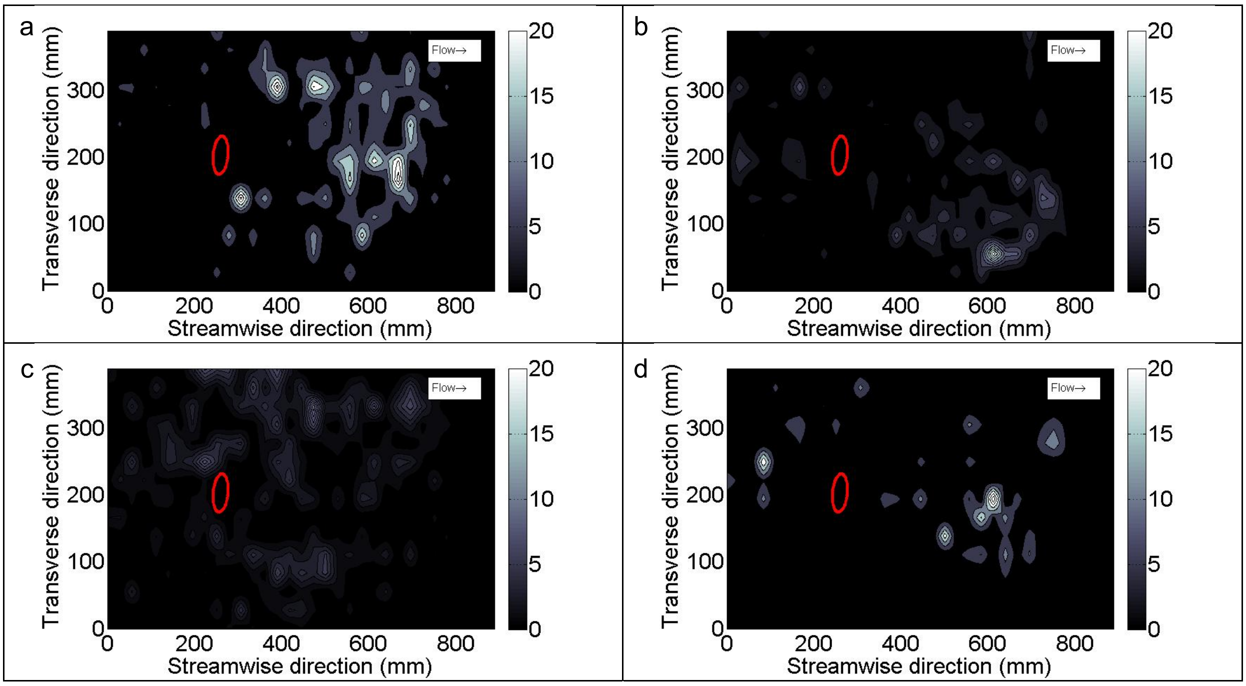

Figure 8. Sediment transport rate ($1x10^{-3}$m3/h for every 30x30mm square section of the bed) over test section with anchor stone position drawn a) Armouring phase (0-35 minutes) b) Prior to cluster formation (35-110 min) c) Cluster fully formed (110-250 min) d) Subsequent to cluster disintegration (250-284 min)

4. CONCLUSIONS

Observations of the cluster show that the cluster fully formed 110 minutes after the anchor stone was deposited on the bed. The wake formed immediately after the anchor stone was deposited, however it decreased in size until the stoss was fully formed, at which point the wake also increased in size to between 0.75 and 1.5 times the anchor stone size. The stoss formed initially due to the sliding of a larger particle to join the anchor stone, thus creating a barrier to sediment movement, and later due to the disintegration of another cluster directly upstream of the anchor stone releasing 3 stones which formed the heart of the stoss. Orientation of the cluster ranged between 0 and 6^{o} from the streamwise direction. Disintegration of the cluster was triggered by the entrainment of a small particle to the side of the anchor stone, followed by a turbulent burst entraining both the most central stone in the stoss and a smaller cluster to the side of the main cluster. The sediment transport rate for the larger size fractions of the bed remained similar throughout the experiment, however, the presence of the cluster slowed the peak rates of local transport on the bed by half, particularly in the section directly downstream of the cluster.

Cluster formation is influenced by many factors, including the physical characteristics of the sediment, viz. grading, shape, and density; and the properties of the surrounding environment, viz. flow rate, relative submergence, flood stage, slope and sediment availability. While these factors are important to the general formation of clusters, the most significant influence on cluster formation appears to be the mechanics of the sediment transport of the surrounding bed. As long as sediment transport is occurring, the cluster is likely to form. The cluster, in turn, influences the properties of sediment transport in the surrounding bed creating a feedback mechanism. This paper provides an insight into the relationship between the cluster and its surroundings in this capacity. The processes developed here will be elaborated on further to observe the behaviour of more clusters under different conditions.

5. ACKNOWLEDGMENTS

The authors would like to acknowledge the assistance and expertise of the lab technicians Geoff Kirby and Jim Luo.

6. REFERENCES

Andrews, E. (1983). *Entrainment of gravel from naturally sorted riverbed material*. Bulletin of the Geological Society of America, 94(10), 1225.

Biggs, B. J. F., Scarsbrook, M. R., Francoeur, S. N., and Duncan, M. J. (1997). *Bed sediment clusters: are they the key to maintaining bio-diversity in New Zealand streams*. Water and Atmosphere, 5(1), 21-23.

Billi, P. (1988). *A note on cluster bedform behaviour in a gravel-bed river*. Catena, 15(5), 473-481.

Blott, S. J., and Pye, K. (2008). *Particle shape: A review and new methods of characterization and classification*. Sedimentology, 55(1), 31-63.

Brayshaw, A. C., ed. (1984). *Characteristics and origin of cluster bedforms in coarse grained alluvial channels*, Canadian Society of Petroleum Geologists, Calgary, Alberta, Canada.

Church, M., Hassan, M. A., and Wolcott, J. F. (1998). *Stabilizing Self-Organized Structures in Gravel-Bed Stream Channels: Field and Experimental Observations*. Water Resour. Res., 34, 3169-3179.

De Jong, C. (1991). *A reappraisal of the significance of obstacle clasts in cluster bedform dispersal*. Earth Surface Processes and Landforms, 16(8), 737-744.

Hassan, M. A., and Reid, I. (1990). *Influence of microform bed roughness elements on flow and sediment transport in gravel bed rivers*. Earth Surface Processes and Landforms, 15(8), 739.

Heays, K., Friedrich, H., and Melville, B. (2010a). *Change of particle size distribution during cluster evolution*. in (Eds) "*International Association of Hydraulic Engineering - Asia Pacific Division*", Auckland, 21-24 February, 2010.

Heays, K., Friedrich, H., and Melville, B. W. (2010b). *Re-evaluation of image analysis for sedimentary process research*. in (Eds) "*International Association of Hydraulic Engineering - Asia Pacific Division*", Auckland, 21-24 February, 2010.

Hendrick, R. R., Ely, L. L., and Papanicolaou, A. N. (2010). *The role of hydrologic processes and geomorphology on the morphology and evolution of sediment clusters in gravel-bed rivers*. Geomorphology, 114(3), 483-496.

Kramer, C. M., and Papanicolaou, A. N. (2005). *The Effects of Relative Submergence on Cluster Formation in Gravel Bed Streams*. in R. Walton (Eds) " *Impacts of Global Climate Change: Proceedings of World Water and Environmental Resources Congress 2005*", Anchorage, May 15–19, 2005.

Oldmeadow, D. F., and Church, M. (2006). *A field experiment on streambed stabilization by gravel structures*. Geomorphology, 78(3-4), 335-350.

Papanicolaou, A. N., and Schuyler, A. (2003). *Cluster evolution and flow-frictional characteristics under different sediment availabilities and specific gravity*. Journal of Engineering Mechanics, 129(10), 1206-1219.

Papanicolaou, A. N., Strom, K., Schuyler, A., and Talebbeydokhti, N. (2003). *The role of sediment specific gravity and availability on cluster evolution*. Earth Surface Processes and Landforms, 28(1), 69-86.

Reid, I., Frostick, L., and Brayshaw, A. (1992). *Microform roughness elements and the selective entrainment and entrapment of particles in gravel-bed rivers*, in P. Billi, J. D. Hey, C. R. Thorne, and P. Tacconi "Dynamics of gravel-bed rivers". John Wiley & Sons Ltd, West Sussex, 253–275.

Strom, K., Papanicolaou, A. N., Evangelopoulos, N., and Odeh, M. (2004). *Microforms in gravel bed rivers: Formation, disintegration, and effects on bedload transport*. Journal of Hydraulic Engineering, 130(6), 554-567.

Strom, K. B. (2006). *Cluster bedforms in mountain rivers*, PhD Thesis, The University of Iowa, Iowa.

Strom, K. B., and Papanicolaou, A. N. (2008). *Morphological characterization of cluster microforms* Sedimentology, 55(1), 137-153.

Wittenberg, L., and Newson, M. D. (2005). *Particle clusters in gravel-bed rivers: An experimental morphological approach to bed material transport and stability concepts*. Earth Surface Processes and Landforms, 30(11), 1351-1368.